

---

# Double Machine Learning Evaluation Under Distribution Shift and Selection Bias

---

Anonymous Author(s)

Affiliation

Address

email

## Abstract

1        Understanding how a model will perform when deployed in unseen environments  
2        is essential to preventing harm when algorithms inform decision-making. Two  
3        important drivers of model performance degradation are (i) *covariate shift* where  
4        the target covariate distribution differs from the source and (ii) *selective labels*  
5        where the observability of outcomes is influenced by the model itself. We study  
6        *pre-deployment* model evaluation under the joint presence of covariate shift and  
7        selective labeling. In particular, we present a double machine learning estimation  
8        procedure for the risk of an arbitrary black-box prediction model for a given loss  
9        function. We show identification of this estimand under standard assumptions,  
10       and derive a bias-corrected estimator based on the influence function of the target  
11       risk. We demonstrate our proposed estimator through controlled synthetic data and  
12       semi-synthetic eICU data experiments, which show that our estimator tracks the  
13       true target risk more accurately than combining standard plug-in approaches.

## 14    1 Introduction

15    Prediction algorithms that perform well within the training environment can degrade when deployed  
16    in new or changing environments. This degradation in performance is particularly consequential  
17    when the algorithms inform decisions that carry high-stakes and directly affect individual welfare  
18    or when the decisions induce changes in the environment. Moreover, the question of understanding  
19    performance degradation when deploying a model in environments that look different than the  
20    training data is inherently one of fairness: if left unaddressed, such models may disproportionately  
21    underperform for demographic groups that are underrepresented in the training data.

22    These concerns are well-supported empirically. As prediction algorithms are increasingly deployed to  
23    aid decision-making, evidence has mounted that performance can degrade significantly in new settings.  
24    For example, medical diagnosis algorithms have been shown to exhibit reduced performance for  
25    demographic groups that are underrepresented in the training data [42, 41, 14, 24, 30, 44]. Similarly,  
26    natural language processing tasks such as clinical text identification and hate speech detection often  
27    underperform on underrepresented subgroups and linguistic varieties [47, 31, 40, 29].

28    A prominent cause of degraded performance is *distribution shift* [34] where the training and deploy-  
29    ment populations differ. One such class of distribution shift is known as *covariate shift* [43] where  
30    the distribution of input features changes while the causal relationship between features and the  
31    output remains constant. In particular, if the performance of the model varies across certain feature  
32    subgroups, covariate shift degrades model performance when the deployment population has a higher  
33    concentration of those features that are harder to predict. Even a model that performs well on average  
34    on the test set can have unpredictable real-world performance as a result of covariate shift [21].

35    A second pertinent source of performance degradation is when outcome labels are not observed  
36    uniformly at random across the population. In many settings, the observability of outcome labels

37 is determined by interventions that are themselves determined by the model’s prediction. This  
38 phenomenon, referred to as the *selective labels problem* [23], impacts both learning and evaluation  
39 because of the selection bias that it imposes on the training data. It is difficult to estimate how the  
40 model would perform under counterfactual outcomes when the corresponding outcome labels are  
41 systematically missing.

42 These two challenges, *covariate shift* and *selective labels*, often coexist in practice when algorithms  
43 are used to aid in high-stakes decision-making. A salient motivating example is the use of *Clinical*  
44 *Decision-making Instruments (CDIs)* which are predictive models used in healthcare settings to  
45 assist with treatment assignment. CDIs use patient features including demographics, symptoms, and  
46 test results, to aid in diagnosis and treatment. CDIs trained on data from large, urban hospitals are  
47 deployed in rural communities where patient populations and medical practices look vastly different.  
48 Moreover, outcome labels are observable only for those patients for which the CDI indicated need for  
49 further testing or observation.

50 In this work, we address the task of pre-deployment model evaluation under covariate shift and  
51 selective labels. Our contributions are

- 52 1. We propose a target risk functional as an estimand to assess model performance in settings  
53 suffering from selective labels and covariate shift.
- 54 2. We demonstrate how to identify the target risk in terms of observable quantities in the data  
55 under a set of standard assumptions, and we characterize the influence function of our target  
56 estimand.
- 57 3. We construct a double machine learning estimator that requires access to only selectively  
58 labeled data from the source environment and unlabeled covariate data from the target  
59 environment. Our approach applies to arbitrary black-box prediction functions and general  
60 loss functions.
- 61 4. We empirically validate our method using synthetic experiments, and we illustrate our  
62 method in a real-world intensive care hospital setting.

## 63 1.1 Background and Related Work

64 **Dataset and Covariate Shift:** Here, we focus on *covariate shift* [43], where the marginal distri-  
65 bution of input features  $P(X)$  changes between the training and deployment environments while  
66 the conditional distribution of the label given features  $P(X|Y)$  remains unchanged<sup>1</sup>. Classic ap-  
67 proaches to mitigating covariate shift rely on importance-weighted estimators [43, 46, 19], though  
68 such methods can suffer high variance. This challenge motivates the use of doubly robust methods  
69 for covariate shift correction [36, 15]. Beyond methods for correcting covariate shift, a growing body  
70 of works addresses the problem of evaluating models under covariate shift [7, 4, 2]. A related line of  
71 work examines whether a given shift is harmful in the first place, as not all shifts necessarily degrade  
72 performance [35, 32, 26].

73 **Selective Labels and Sample Selection Bias:** The *selective labels* problem arises when a model’s  
74 predictions determine whether outcomes are observed. In such settings, outcome labels are available  
75 only for a biased sample of the overall population, which undermines learning and evaluation. In credit  
76 scoring mechanisms, an analogous challenge known as *rejection inference* is commonly addressed by  
77 training and evaluating models on only the labeled subset of samples [3, 1]; This approach has raised  
78 fairness and bias concerns [12, 13].

79 Another class of methods estimates the outcome for unlabeled samples [8, 5]. Alternatively, others  
80 leverage heterogeneity across decision-makers to correct the model and its evaluation [20, 6]. Other  
81 approaches include data augmentation procedures to acquire outcomes for subpopulations that are  
82 underrepresented in labeled samples [9] or directly incorporating consideration for downstream  
83 decision-making while training and evaluating models [11].

84 **Double Machine Learning** Double machine learning, also known as doubly robust estimation,  
85 is an estimation approach for settings with incomplete data that has become popular due to the  
86 desirable properties of the resulting estimators. In parametric settings, doubly robust estimators

---

<sup>1</sup>See, e.g., [34, 25, 28] for surveys on distribution shift more broadly.

87 remain consistent if either the propensity score or outcome model are correctly specified [38, 37, 22].  
 88 Such estimators enjoy fast rates of convergence in nonparametric settings [16] and have been used  
 89 for estimation in settings closely related to selective labels and dataset shift, e.g., policy learning [10],  
 90 covariate shift [7, 4, 2], and the challenge of data missing not at random [27, 45].

## 91 2 Problem Setting

92 We consider the problem of evaluating a fixed prediction model under the joint presence of covariate  
 93 shift and selective labeling. Suppose that we observe  $n$  independent and identically distributed (i.i.d)  
 94 draws

$$Z := (X, R, RD, RY). \quad (1)$$

95 Each sample  $Z$  comprises a covariate vector  $X \in \mathcal{X} \subset \mathbb{R}^d$ , a domain indicator  $R \in \{0, 1\}$ , a binary  
 96 treatment  $D \in \{0, 1\}$ , and a scalar outcome  $Y \in \mathbb{R}$ . The label  $R = 1$  designates units from the *source*  
 97 population governed by law  $P_S$  while the label  $R = 0$  designates units from the *target* population  
 98 governed by  $P_T$ ; A binary treatment  $D \in \{0, 1\}$  records an intervention of interest, and  $Y$  is the  
 99 associated outcome.

100 We adopt the potential outcomes framework [39] wherein each individual is associated with counter-  
 101 factual outcomes  $Y(1)$  and  $Y(0)$  corresponding to the outcomes under treatment and no treatment,  
 102 respectively. The observed outcome  $Y$  is determined by the treatment assignment:

$$Y = D \cdot Y(1) + (1 - D) \cdot Y(0). \quad (2)$$

103 Due to selective labeling,  $Y$  is only observed for units for which  $R = 1$  and  $D = 1$ . In other words,  
 104 we observe labeled outcomes only for treated individuals originating from the source distribution.

105 Let  $P_S(X) := \mathbb{P}(X|R = 1)$  and  $P_T(X) := \mathbb{P}(X|R = 0)$  denote the source and target covariate  
 106 distributions, respectively, with corresponding probability density functions  $p_S(x)$  and  $p_T(x)$ . We  
 107 denote by  $\mathbb{E}_S$  and  $\mathbb{E}_T$  the expectation taken with respect to laws  $P_S$  and  $P_T$ , respectively.

108 Our objective is to assess the accuracy of a fixed prediction model  $f : \mathcal{X} \rightarrow \mathbb{R}$ , which has been  
 109 trained to estimate the treated potential outcome  $Y(1)$ . Specifically, we aim to evaluate the model  
 110 under the target covariate distribution  $P_T$ . For a given loss function  $\ell : \mathbb{R} \times \mathbb{R} \rightarrow \mathbb{R}_{\geq 0}$  (e.g., squared  
 111 loss), the estimand of interest is the *target risk*:

$$\psi := \mathbb{E}_T[\ell(f(X), Y(1))]. \quad (3)$$

## 112 3 Identification and Estimation of the Target Risk

113 To describe the identification and estimation of  $\psi$ , it is convenient to introduce additional notation.  
 114 We use  $L := \ell(f(X), Y)$  as shorthand notation for the loss under  $f$ . Also define the following  
 115 *nuisance functions*:

$$\pi(X) := \mathbb{P}(D = 1, R = 1|X), \quad \rho := \mathbb{P}(R = 0), \quad g(X) := \mathbb{P}(R = 0|X), \quad (4)$$

116 and

$$\mu(X) = \mathbb{E}[L|X, R = 1, D = 1], \quad (5)$$

117 the conditional mean loss among treated source units. Estimation of  $\psi$  is complicated by the fact  
 118 that  $Y(1)$  is unobserved in the target domain ( $R = 0$ ) and because, in the source domain, it is only  
 119 observed for treated individuals ( $D = 1, R = 1$ ). To ensure identifiability, we impose standard  
 120 assumptions from causal inference and transfer learning:

121 **Assumption 1** (No unobserved confounding).  $Y(d) \perp\!\!\!\perp D|X \quad \forall d \in \{0, 1\}$ .

122 **Assumption 2** (Covariate Shift).  $\mathbb{P}(Y(d)|X, R = 1) = \mathbb{P}(Y(d)|X, R = 0) \quad \forall d \in \{0, 1\}$ .

123 **Assumption 3** (Positivity). *There exists  $\varepsilon > 0$  such that  $\mathbb{P}(D = 1, R = 1|X) > \varepsilon$  almost surely.*

124 **Assumption 4** (Bounded density ratio). *There exists  $C < \infty$  such that  $\frac{dP_T}{dP_S}(x) \leq C \quad \forall x \in \mathcal{X}$ .*

125 Assumptions 1-4 enable identification of the target risk (3) from observable data. Intuitively, these  
 126 conditions require that (i) there are no unmeasured confounders, (ii) the relationship between covari-  
 127 ates and outcomes is invariant across the source and target domains, (iii) every covariate profile admits  
 128 a positive probability of treatment, and (iv) the source and target distributions' supports overlap  
 129 sufficiently.

130 **Proposition 5** (Identification of the Target Risk). *Under Assumptions 1-4 and with nuisance functions*  
 131  $\pi, \rho, g,$  and  $\mu$  as defined in (4) and (5), the target risk  $\psi$  is identifiable from the observed data as

$$\psi = \mathbb{E}_T[\mu(X)] = \mathbb{E}_S \left[ \frac{p_T(X)}{p_S(X)} \cdot \frac{D \cdot R}{\pi(X)} L \right].$$

132 This result is the foundation of our proposed estimation procedure. The first equality provides a  
 133 convenient expression of the estimand that enables our derivation of an influence function and the  
 134 double machine learning estimator that it motivates. The second equality gives an alternative expres-  
 135 sion for our estimand that shows it can be identified from the source distribution by a reweighting  
 136 procedure that resembles inverse propensity weighting (IPW) methods with an additional density  
 137 ratio correction. A proof of this result is provided in Appendix A.1.

### 138 3.1 Estimation of the Target Risk

139 Next, we use the identification established in Proposition 5 to develop estimators for  $\psi$  based on the  
 140 functional's influence function. Let  $\mathcal{P}$  denote the nonparametric model defined by Assumptions 1-4.

141 **Proposition 6** (Target Risk Influence Function). *For every  $\mathbb{P} \in \mathcal{P}$ , the map  $\psi : \mathbb{P} \rightarrow \mathbb{R}$  admits the*  
 142 *expansion*

$$\psi(\bar{\mathbb{P}}) - \psi(\mathbb{P}) = \int \varphi(z; \bar{\mathbb{P}}) d(\bar{\mathbb{P}} - \mathbb{P})(z) + R_2(\mathbb{P}, \bar{\mathbb{P}}), \quad (6)$$

143 with influence function

$$\varphi(Z; \mathbb{P}) = \frac{RD}{\pi(X)} \frac{g(X)}{\rho} (L - \mu(X)) + \frac{1 - R}{\rho} (\mu(X) - \psi(\mathbb{P})). \quad (7)$$

144 The remainder  $R_2(\mathbb{P}, \bar{\mathbb{P}})$  comprises terms that are second order in the estimation errors of  $(\mu, \pi, g)$   
 145 and first order in the estimation error of  $\rho$ .

146 Proposition 6 establishes the influence function representation and remainder term expansion of the  
 147 estimand  $\psi$ . The result follows from semiparametric efficiency theory, and is proved in detail in  
 148 Appendix A.2.1. We outline the main steps of the proof here.

149 First, we identify a valid candidate influence function using established results on the influence  
 150 functions of conditional expectations and densities (see, e.g., [18]). Next, we evaluate the efficiency  
 151 of the candidate influence function by establishing an expansion of  $\psi$  with respect to an arbitrarily  
 152 perturbed distribution in  $\mathcal{P}$ .

### 153 3.2 Our double machine learning estimator of target risk

154 Motivated by the influence function derived in Proposition 6, we next construct a double machine  
 155 learning estimator for the target risk  $\psi$ . Double machine learning, also known as one-step estimators  
 156 or doubly-robust estimators, is a popular method for constructing estimators in settings with missing  
 157 data such as causal inference [17]. To avoid overfitting due to nuisance parameter estimation, we  
 158 employ standard sample-splitting techniques that retain the independence of nuisance parameter  
 159 estimates by partitioning the data into independent folds. See Appendix B.1 for a detailed description  
 160 of this procedure.

161 Formally, the estimator motivated by (7) is given by:

$$\hat{\psi} = \frac{1}{n} \frac{1}{\hat{\rho}} \sum_{i=1}^n \left[ \frac{R_i D_i}{\hat{\pi}_i} \hat{g}(X_i) (L_i - \hat{\mu}(X_i)) + (1 - R_i) \hat{\mu}(X_i) \right]. \quad (8)$$

162 where  $\hat{\pi}, \hat{g}$  and  $\hat{\mu}$  denote cross-fitted nuisance estimators, and  $\hat{\rho}$  is the empirical estimator of  $\rho$ .

163 The estimator (8) enjoys the *double robustness* property: In a parametric setting, it is consistent if  
 164 either (i) the conditional mean  $\mu(X)$  is correctly specified or (ii) the propensity score  $\pi(X)$  and the  
 165 density ratio  $g(X)$  are correctly specified. If we are using non-parametric methods to estimate the  
 166 nuisance functions, the estimator is  $\sqrt{n}$ -consistent and asymptotically normal under sample-splitting  
 167 and  $n^{1/4}$  convergence in the nuisance function estimation error.<sup>2</sup>

<sup>2</sup>This contrasts to standard methods like the plug-in or inverse probability weighting approach that would require  $\sqrt{n}$  convergence in the nuisance function estimation error.

## 168 4 Experiments

### 169 4.1 Synthetic Experiments

170 **Synthetic Data Generation:** We evaluate and compare our proposed estimators via a synthetic  
 171 experiment through a procedure that simulates the combined setting of covariate shift and selective  
 172 labeling. We generate  $n_S$  source samples  $X_i^{(S)} \sim \mathcal{N}(\mu_S, \Sigma_S)$  and  $n_T$  target samples  $X_i^{(T)} \sim$   
 173  $\mathcal{N}(\mu_T, \Sigma_T)$ . By varying  $\mu_S \neq \mu_T$  and/or  $\Sigma_S \neq \Sigma_T$ , we simulate covariate shift between source and  
 174 target distributions.

175 **Treatment and Outcome Models:** For each source sample  $X_i^{(S)}$ , we compute treatment proba-  
 176 bilities via a logistic regression model  $\pi(X_i) = \sigma(\alpha^\top X_i)$ , where  $\sigma(\cdot)$  is the sigmoid function and  
 177  $\alpha = c \cdot \mathbb{1}_d$  for a constant  $c$  unless otherwise noted. We then sample treatment indicators  $D_i \sim$   
 178 Bernoulli( $\pi(X_i)$ ), simulating a selection policy that depends on covariates. Then, we generate po-  
 179 tential outcomes for the treated units in the source distribution  $Y(1)_i \sim \text{Bernoulli}(\text{sigmoid}(\beta^\top X_i))$   
 180 where  $\beta \in \mathbb{R}^d$  is taken to be  $C \cdot \mathbb{1}_d$  for an appropriate scaling factor  $C$  unless otherwise noted. To  
 181 introduce noise, we randomly flip the binary outcomes with probability  $\gamma \in (0, 1)$ , taking  $\gamma = 0.1$   
 182 unless otherwise noted. Then we simulate selective labeling by setting  $Y_i = \text{NA}$  for all units with  
 183  $D_i = 0$ , meaning outcomes are only observed for treated units.

184 **Model Training:** We randomly split the observed subset of the source data (i.e., units with  $D_i = 1$ )  
 185 into 80% training and 20% test subsets. We train a logistic model on the training subset to predict  
 186 the outcome  $Y(1)$  from covariates  $X$ . This model  $f$  is used to estimate  $\mathbb{E}[Y(1)|X]$ . We evaluate the  
 187 mean squared error (MSE) of predictions on the held-out source test set.

188 **Nuisance Parameter Estimation:** To account for covariate shift, we fit a domain classifier (logistic  
 189 regression) to distinguish between source and target samples, assigning the label  $R = 1$  to the source  
 190 and  $R = 0$  to the target:

$$\hat{w}(x) = \frac{1 - \hat{\mathbb{P}}(R = 1|X = x)}{\max\{\hat{\mathbb{P}}(R = 1), \varepsilon\}}$$

191 where  $\varepsilon$  is a small positive constant to avoid division by zero. This yields an estimate of the  
 192 density ratio  $w(x) = \frac{p_T(x)}{p_S(x)}$ . Next, we fit a logistic regression model to estimate the propensity  
 193 score:  $\hat{\pi}(x) = \hat{\mathbb{P}}(D = 1|X = x, R = 1)$  using logistic regression trained on the source samples  
 194 which we evaluate on both the source and target data. Next, we compute the squared error losses  
 195  $L_i = (f(X_i) - Y_i)^2$  for the subset of samples from the source distribution that are treated and have  
 196 observable outcomes  $Y_i$ . Using these observed  $(L_i, X_i)$  pairs, we train a random forest regressor  
 197  $\hat{\mu}(x)$  to estimate the expected loss  $\mathbb{E}[L|X = x]$ .

198 **Compute Naïve (Plug-in) Estimator:** The plug-in estimator computes the average predicted  
 199 squared loss on the observed treated source data, reweighting by the estimated density ratio  $\hat{w}(x)$  and  
 200 the inverse propensity weights  $1/\hat{\pi}(x)$  to account for both the covariate shift and selective labels. We  
 201 compute:  $\hat{\psi}_{\text{plugin}} = \frac{1}{n_{RD}} \sum_{i=1}^{n_{RD}} \frac{R_i \cdot D_i \cdot \hat{w}(X_i) \cdot L_i}{\hat{\pi}(X_i)}$  where  $n_{RD} = \sum_{i=1}^{n_P} R_i \cdot D_i$ , the number of labeled  
 202 samples in the source distribution.

203 **Compute DML Estimator:** We also compute the DML estimator for the target risk:  $\hat{\psi}_{\text{DML}} =$   
 204  $\frac{1}{n} \sum_{i=1}^n \left( \frac{R_i \cdot D_i \cdot \hat{w}(X_i)}{\hat{\pi}(X_i)} (L_i - \hat{\mu}(X_i)) + \frac{1-R_i}{\hat{P}(R=0)} \hat{\mu}(X_i) \right)$  where  $R_i$  is the domain indicator,  $D_i$  is the  
 205 treatment indicator, and  $\hat{P}(R = 0)$  denotes an empirical estimate of drawing from the target  
 206 distribution.

207 **Estimate True Risk in Target with MC:** To estimate the ground truth target risk, we simulate an  
 208 oracle dataset of  $n_{\text{oracle}}$  samples from the target distribution. For each sample  $X_i^{(T)} \sim \mathcal{N}(\mu_T, \Sigma_T)$ ,  
 209 we generate a potential outcome using the same outcome model and again flip outcomes randomly  
 210 with probability  $\gamma$  to introduce noise. The ground truth risk estimate is then computed as the mean

211 squared error:  $\psi_{\text{oracle}} = \frac{1}{n_{\text{oracle}}} \sum_{i=1}^{n_{\text{oracle}}} (f(X_i) - Y_i(1))^2$ . This serves as a benchmark against which  
 212 we evaluate our estimators  $\hat{\psi}_{\text{DML}}$  and  $\hat{\psi}_{\text{plug-in}}$ .

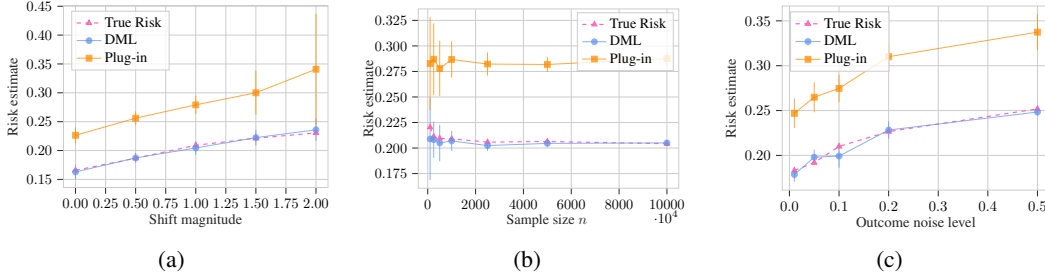


Figure 1: Results of synthetic experiment comparing DML and plug-in estimators for risk with the true risk under increasing covariate shift magnitude, increasing sample size, and increasing noise in the outcome model. (a) We increase the magnitude of  $|\mu_S - \mu_T|$  along the direction of the true outcome model coefficients and report the average estimated risk over 30 trials for the plug-in and DML estimators, with error bars denoting standard deviations. (b) We increase the sample size  $n = n_T = n_S$  and report the estimated risk averaged over 30 trials with error bars denoting standard deviations. (c) We increase the level of random outcome noise  $\gamma$  (i.e., the probability of flipping the binary outcome of our outcome model) and evaluate the average estimated risk over 30 trials with error bars denoting standard deviations.

213 **Synthetic Experiment Results** In Figure 1a, we see that the DML estimator consistently tracks the  
 214 true target risk more accurately across all covariate shift magnitudes where the shift is with respect to  
 215 the mean of the Gaussian covariate distributions, while the plug-in estimator becomes increasingly  
 216 biased as the shift grows. In Figure 1b, we see that the both the DML and plug-in estimators improve  
 217 as sample size increases, while the DML estimator aligns closely with the true risk while the plug-in  
 218 estimator appears biased. In Figure 1c, we see that both estimators capture the risk trend as outcome  
 219 noise increases while the DML estimator once again tracks the target risk more accurately.

## 220 4.2 Semi-Synthetic Experiments

221 It is well-known that dataset shifts “in the wild” are often more complicated and difficult to address  
 222 than shifts simulated in controlled, synthetic experiments [21]. This motivates experimentation that  
 223 incorporates real covariates and identifies natural covariate shifts rather than simulating such shifts as  
 224 our first set of experiments did. To accomplish this task, we access data from the eICU Collaborative  
 225 Research Database [33] which includes intensive care unit (ICU) data from multiple treatment centers  
 226 across the United States. We leverage the fact that the data include multiple treatment sites to simulate  
 227 the setting where a model is trained on a population that differs in demographic makeup from the  
 228 population on which it is to be deployed. By nature of the selective labels problem, we must still  
 229 rely on the treatment and outcome models previously described in the fully synthetic experiment  
 230 procedure since the data include only treated and labeled patients.

231 **eICU Data:** The eICU Collaborative Research Database [33] includes de-identified individual-  
 232 level electronic health records from over 200,000 admissions to ICUs across multiple hospitals in  
 233 the United States. Here, we focus on admission-level patient demographic and health data. We  
 234 extract gender, ethnicity and age data, vitals including admission height, weight, and body mass  
 235 index, clinical unit type (e.g., medical, surgical), and hospital ID. We one-hot-encode all categorical  
 236 variables and impute missing values in continuous features with the median. All continuous features  
 237 are standardized with Z-score normalization for computational tractability.

238 **Constructing Covariate Shift:** To simulate distribution shift that captures real-world complexity,  
 239 we use patient data from a selected training hospital to construct the training environment and use  
 240 all patient data from the remaining hospitals to construct the target environment. In particular, we  
 241 select training hospitals that look systematically different from the general population in age and  
 242 race/ethnicity. Figures Figure 2 and 3 compare the age and ethnicity covariate distributions of the  
 243 identified source and target hospitals, respectively.

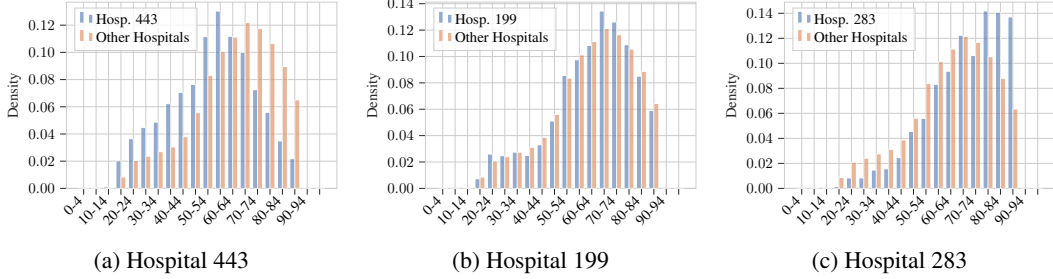


Figure 2: Comparison of age across hospitals in the eICU data. (a) Hospital 443 tends to have younger patients than other hospitals; (b) Hospital 199 has a typical age distribution; and (c) Hospital 283 tends to have older patients.

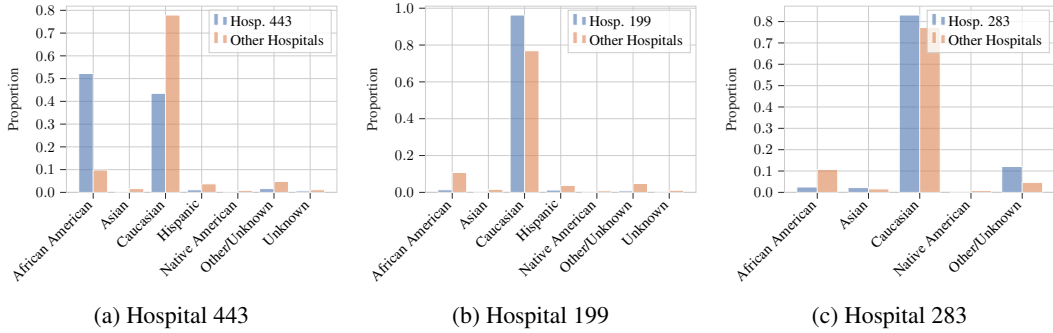


Figure 3: Comparison of ethnicity covariates across hospitals. (a) Hospital 443 tends to have more African American patients and fewer caucasian patients than other hospitals; (b) Hospital 199 tends to have more caucasian patients; (c) Hospital 283 tends to have a larger portion of patients with ethnicity unknown or labeled as “other”.

**Semi-Synthetic Experiment Procedure:** Using actual patient covariates, we simulate models and outcomes by the same procedure as the purely synthetic experiments. We take  $n_T$  to be the number of units in the training hospital. Then, we randomly select  $n_T$  samples from the remaining hospitals to represent the unlabeled samples from the target setting. In other words, we take  $n_S = n_T$ . The rest of the samples are used to construct the oracle estimate of risk. Treatment is assigned using a draw from a Bernoulli distribution with probabilities determined by the patient features:

$$\pi(X) = \sigma(X^\top \alpha)$$

244 where  $\alpha$  in this case takes a small constant  $c$ . The outcome is similarly generated via Bernoulli  
 245 draws with probability determined by  $X^\top \beta$  where  $\beta \in \mathbb{R}^d$  is taken to be a randomly sampled and  
 246 normalized vector of coefficients for each iteration. Once again, we simulate outcome noise by  
 247 flipping a proportion  $\gamma$  of the generated outcomes. The model fitting and estimator construction  
 248 remains unchanged from the synthetic experiments. To estimate the true risk of deploying the model  
 249 on the target population, we construct a Monte Carlo estimate of the risk using the remaining unused  
 250 samples.

251 **Semi-Synthetic Experiment Results:** We use three different hospitals as the training center  
 252 where each varies notably from the rest of the hospitals in its distribution of age, ethnicity, or both,  
 253 as depicted in Figure 2 and Figure 3. We conduct experiments of the estimators under increasing  
 254 noise in the outcome model as well as increasing propensity strength (increasing norm of  $\alpha$ ) and  
 255 increasing effect size (increasing norm of  $\beta$ ). In Figure 4, we see that the DML estimator once  
 256 again tracks the true risk more closely. Interestingly, here we observe behavior where the plug-in  
 257 estimator both overestimates and underestimates the true risk. While *underestimation* of the true  
 258 risk is particularly consequential in the medical contexts, *overestimation* is also relevant when data  
 259 acquisition and model training are costly. In Figure 5, we see that increasing the propensity strength  
 260 has little systematic effect on either estimator, though the DML estimator once again aligns with the

261 true risk more closely. Finally, in Figure 6, we see that increasing the effect size decreases the risk  
 262 estimate of both estimators as well as the true risk, where the DML estimator appears to increasingly  
 263 diverge from the true risk estimate under increasing effect size in Figure 6a.

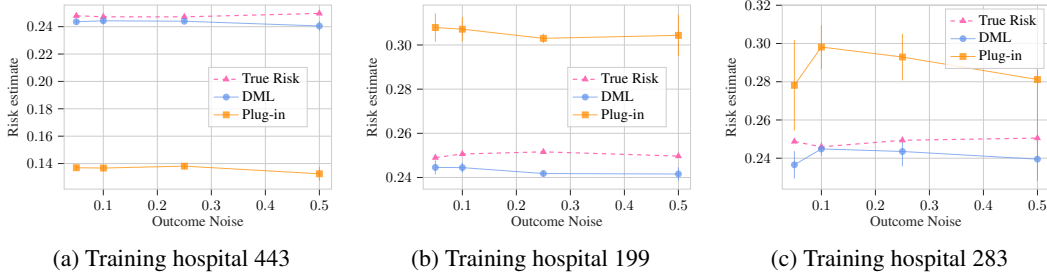


Figure 4: Comparison of DML and plug-in estimators with true risk across increasing noise levels in the outcome model  $\gamma \in (0.05, 0.5)$  across three different training hospital configurations. The error bars represent standard deviation over 5 iterations. Our DML method more closely tracks the true risk than the plug-in estimator.

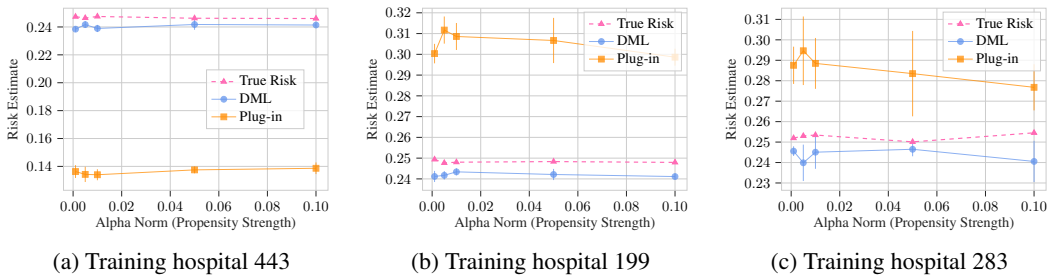


Figure 5: Comparison of DML and plug-in estimators with true risk across increasing norm in the propensity parameter  $\alpha$  and across three different training hospital configurations. The error bars represent standard deviations over 5 iterations. Our DML method more closely tracks the true risk than the plug-in estimator.

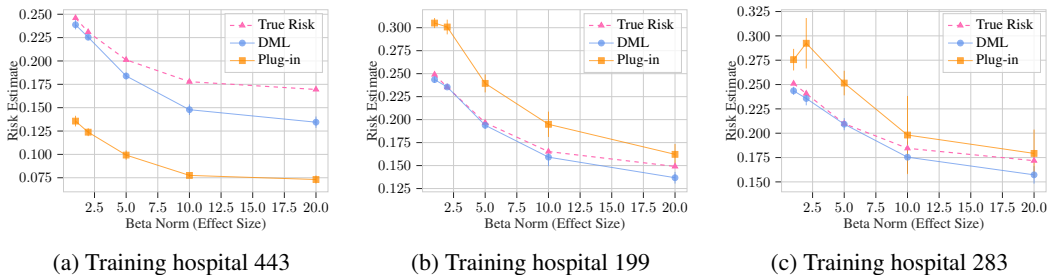


Figure 6: Comparison of DML and plug-in estimators with true risk across increasing norm in effect size parameter  $\beta$  and across three different training hospital configurations. The error bars represent standard deviations over 5 iterations. Our DML method more closely tracks the true risk than the plug-in estimator.

## 264 5 Conclusion

265 We studied the problem of pre-deployment model evaluation under the joint presence of covariate  
 266 shift and selective labels. We formalized the target risk as an estimand that captures a model's  
 267 expected performance in the deployment environment, and established conditions under which it  
 268 is identifiable from observable data. We derived an influence function representation of the target



269 risk and used it to construct a doubly robust, double machine learning estimator. Our estimator uses  
270 selectively labeled source data and unlabeled data from the target distribution.

271 Through synthetic and semi-synthetic experiments, we showed that our estimator more accurately  
272 tracks the true target risk in comparison with standard plug-in procedures. These results highlight the  
273 importance of developing tools that can account for multiple coexisting data challenges. In particular,  
274 the combination of covariate shift and selective labels, each of which has been studied extensively in  
275 isolation, poses distinct difficulties and is likely to arise in high-stakes domains such as healthcare.

276 Our work also points to several directions for future work. Relaxing the assumption of no unmeasured  
277 confounding and constructing similar estimators for other types of dataset shift would provide  
278 insight into other important domains where prediction algorithms inform decisions. In addition,  
279 many of the environments where our framework is relevant are also those in which it is natural to  
280 desire fairness-aware evaluation. Adapting our approach to explicitly consider fairness, e.g., by  
281 evaluating performance gaps across subgroups, would further strengthen the reliability of algorithmic  
282 decision-making.

## 283 References

- 284 [1] R. Berk, L. Sherman, G. Barnes, E. Kurtz, and L. Ahlman. Forecasting murder within a  
285 population of probationers and parolees: a high stakes application of statistical learning. *Journal*  
286 *of the Royal Statistical Society Series A: Statistics in Society*, 172(1):191–211, 2009.
- 287 [2] J. Białek, W. Kuberski, N. Perrakis, and A. Bifet. Estimating model performance under covariate  
288 shift without labels. *arXiv preprint arXiv:2401.08348*, 2024.
- 289 [3] L. Blattner and S. Nelson. How costly is noise? data and disparities in consumer credit. *arXiv*  
290 *preprint arXiv:2105.07554*, 2021.
- 291 [4] T. T. Cai, H. Namkoong, and S. Yadlowsky. Diagnosing model performance under distribution  
292 shift. *arXiv preprint arXiv:2303.02011*, 2023.
- 293 [5] T. Chang and J. Wiens. From biased selective labels to pseudo-labels: an expectation-  
294 maximization framework for learning from biased decisions. *arXiv preprint arXiv:2406.18865*,  
295 2024.
- 296 [6] J. Chen, Z. Li, and X. Mao. Learning under selective labels with data from heterogeneous  
297 decision-makers: An instrumental variable approach. *arXiv preprint arXiv:2306.07566*, 2023.
- 298 [7] L. Chen, M. Zaharia, and J. Y. Zou. Estimating and explaining model performance when  
299 both covariates and labels shift. *Advances in Neural Information Processing Systems*, 35:  
300 11467–11479, 2022.
- 301 [8] A. Coston, A. Mishler, E. H. Kennedy, and A. Chouldechova. Counterfactual risk assessments,  
302 evaluation, and fairness. In *Proceedings of the 2020 conference on fairness, accountability, and*  
303 *transparency*, pages 582–593, 2020.
- 304 [9] M. De-Arteaga, A. Dubrawski, and A. Chouldechova. Learning under selective labels in the  
305 presence of expert consistency. *arXiv preprint arXiv:1807.00905*, 2018.
- 306 [10] M. Dudík, J. Langford, and L. Li. Doubly robust policy evaluation and learning. *arXiv preprint*  
307 *arXiv:1103.4601*, 2011.
- 308 [11] D. Ensign, S. A. Friedler, S. Neville, C. Scheidegger, and S. Venkatasubramanian. Decision  
309 making with limited feedback: Error bounds for recidivism prediction and predictive policing.  
310 *Proceedings of FAT/ML 2017*, 2017.
- 311 [12] A. Fuster, P. Goldsmith-Pinkham, T. Ramadorai, and A. Walther. Predictably unequal? the  
312 effects of machine learning on credit markets. *The Journal of Finance*, 77(1):5–47, 2022.
- 313 [13] N. Kallus and A. Zhou. Residual unfairness in fair machine learning from prejudiced data. In  
314 *International Conference on Machine Learning*, pages 2439–2448. PMLR, 2018.

- 315 [14] L. Kamulegeya, J. Bwanika, M. Okello, D. Rusoke, F. Nassiwa, W. Lubega, D. Musinguzi, and  
316 A. Börve. Using artificial intelligence on dermatology conditions in uganda: A case for diversity  
317 in training data sets for machine learning. *African Health Sciences*, 23(2):753–63, 2023.
- 318 [15] M. Kato, K. Matsui, and R. Inokuchi. Double debiased covariate shift adaptation robust to  
319 density-ratio estimation. *arXiv preprint arXiv:2310.16638*, 2023.
- 320 [16] E. H. Kennedy. Semiparametric theory and empirical processes in causal inference. In *Statistical*  
321 *causal inferences and their applications in public health research*, pages 141–167. Springer,  
322 2016.
- 323 [17] E. H. Kennedy. Semiparametric doubly robust targeted double machine learning: a review.  
324 *arXiv preprint arXiv:2203.06469*, 2022.
- 325 [18] E. H. Kennedy, S. Balakrishnan, and L. Wasserman. Semiparametric counterfactual density  
326 estimation. *Biometrika*, 110(4):875–896, 2023.
- 327 [19] M. Kimura and H. Hino. A short survey on importance weighting for machine learning. *arXiv*  
328 *preprint arXiv:2403.10175*, 2024.
- 329 [20] J. Kleinberg, H. Lakkaraju, J. Leskovec, J. Ludwig, and S. Mullainathan. Human decisions and  
330 machine predictions. *The quarterly journal of economics*, 133(1):237–293, 2018.
- 331 [21] P. W. Koh, S. Sagawa, H. Marklund, S. M. Xie, M. Zhang, A. Balsubramani, W. Hu, M. Ya-  
332 sunaga, R. L. Phillips, I. Gao, et al. Wilds: A benchmark of in-the-wild distribution shifts. In  
333 *International conference on machine learning*, pages 5637–5664. PMLR, 2021.
- 334 [22] M. J. Laan and J. M. Robins. *Unified methods for censored longitudinal data and causality*.  
335 Springer, 2003.
- 336 [23] H. Lakkaraju, J. Kleinberg, J. Leskovec, J. Ludwig, and S. Mullainathan. The selective labels  
337 problem: Evaluating algorithmic predictions in the presence of unobservables. In *Proceedings*  
338 *of the 23rd ACM SIGKDD International Conference on Knowledge Discovery and Data Mining*,  
339 pages 275–284, 2017.
- 340 [24] A. J. Larrazabal, N. Nieto, V. Peterson, D. H. Milone, and E. Ferrante. Gender imbalance in  
341 medical imaging datasets produces biased classifiers for computer-aided diagnosis. *Proceedings*  
342 *of the National Academy of Sciences*, 117(23):12592–12594, 2020.
- 343 [25] J. Liu, Z. Shen, Y. He, X. Zhang, R. Xu, H. Yu, and P. Cui. Towards out-of-distribution  
344 generalization: A survey. *arXiv preprint arXiv:2108.13624*, 2021.
- 345 [26] N. Mallinar, A. Zane, S. Frei, and B. Yu. Minimum-norm interpolation under covariate shift.  
346 *arXiv preprint arXiv:2404.00522*, 2024.
- 347 [27] W. Miao and E. J. Tchetgen Tchetgen. On varieties of doubly robust estimators under missing-  
348 ness not at random with a shadow variable. *Biometrika*, 103(2):475–482, 2016.
- 349 [28] J. G. Moreno-Torres, T. Raeder, R. Alaiz-Rodríguez, N. V. Chawla, and F. Herrera. A unifying  
350 view on dataset shift in classification. *Pattern recognition*, 45(1):521–530, 2012.
- 351 [29] M. Mozafari, R. Farahbakhsh, and N. Crespi. A bert-based transfer learning approach for hate  
352 speech detection in online social media. In *International conference on complex networks and*  
353 *their applications*, pages 928–940. Springer, 2019.
- 354 [30] Z. Obermeyer, B. Powers, C. Vogeli, and S. Mullainathan. Dissecting racial bias in an algorithm  
355 used to manage the health of populations. *Science*, 366(6464):447–453, 2019.
- 356 [31] J. H. Park, J. Shin, and P. Fung. Reducing gender bias in abusive language detection. *arXiv*  
357 *preprint arXiv:1808.07231*, 2018.
- 358 [32] A. Podkopaev and A. Ramdas. Tracking the risk of a deployed model and detecting harmful  
359 distribution shifts. *arXiv preprint arXiv:2110.06177*, 2021.

- 360 [33] T. J. Pollard, A. E. Johnson, J. D. Raffa, L. A. Celi, R. G. Mark, and O. Badawi. The eicu  
361 collaborative research database, a freely available multi-center database for critical care research.  
362 *Scientific data*, 5(1):1–13, 2018.
- 363 [34] J. Quiñonero-Candela, M. Sugiyama, A. Schwaighofer, and N. D. Lawrence. *Dataset shift in*  
364 *machine learning*. Mit Press, 2022.
- 365 [35] S. Rabanser, S. Günnemann, and Z. Lipton. Failing loudly: An empirical study of methods for  
366 detecting dataset shift. *Advances in Neural Information Processing Systems*, 32, 2019.
- 367 [36] S. Reddi, B. Poczos, and A. Smola. Doubly robust covariate shift correction. In *Proceedings of*  
368 *the AAAI conference on artificial intelligence*, volume 29, 2015.
- 369 [37] J. M. Robins and A. Rotnitzky. Semiparametric efficiency in multivariate regression models  
370 with missing data. *Journal of the American Statistical Association*, 90(429):122–129, 1995.
- 371 [38] J. M. Robins, A. Rotnitzky, and L. P. Zhao. Estimation of regression coefficients when some  
372 regressors are not always observed. *Journal of the American statistical Association*, 89(427):  
373 846–866, 1994.
- 374 [39] D. B. Rubin. Causal inference using potential outcomes: Design, modeling, decisions. *Journal*  
375 *of the American statistical Association*, 100(469):322–331, 2005.
- 376 [40] M. Sap, D. Card, S. Gabriel, Y. Choi, and N. A. Smith. The risk of racial bias in hate speech  
377 detection. In *Proceedings of the 57th annual meeting of the association for computational*  
378 *linguistics*, pages 1668–1678, 2019.
- 379 [41] L. Seyyed-Kalantari, G. Liu, M. McDermott, I. Y. Chen, and M. Ghassemi. Chexclusion:  
380 Fairness gaps in deep chest x-ray classifiers. In *BIOCOMPUTING 2021: proceedings of the*  
381 *Pacific symposium*, pages 232–243. World Scientific, 2020.
- 382 [42] L. Seyyed-Kalantari, H. Zhang, M. B. McDermott, I. Y. Chen, and M. Ghassemi. Underdiagnosis  
383 bias of artificial intelligence algorithms applied to chest radiographs in under-served patient  
384 populations. *Nature medicine*, 27(12):2176–2182, 2021.
- 385 [43] H. Shimodaira. Improving predictive inference under covariate shift by weighting the log-  
386 likelihood function. *Journal of statistical planning and inference*, 90(2):227–244, 2000.
- 387 [44] A. Vaidya, R. J. Chen, D. F. Williamson, A. H. Song, G. Jaume, Y. Yang, T. Hartvigsen, E. C.  
388 Dyer, M. Y. Lu, J. Lipkova, et al. Demographic bias in misdiagnosis by computational pathology  
389 models. *Nature Medicine*, 30(4):1174–1190, 2024.
- 390 [45] X. Wang, R. Zhang, Y. Sun, and J. Qi. Doubly robust joint learning for recommendation on data  
391 missing not at random. In *International Conference on Machine Learning*, pages 6638–6647.  
392 PMLR, 2019.
- 393 [46] M. Yamada, T. Suzuki, T. Kanamori, H. Hachiya, and M. Sugiyama. Relative density-ratio  
394 estimation for robust distribution comparison. *Neural computation*, 25(5):1324–1370, 2013.
- 395 [47] H. Zhang, A. X. Lu, M. Abdalla, M. McDermott, and M. Ghassemi. Hurtful words: quantifying  
396 biases in clinical contextual word embeddings. In *proceedings of the ACM Conference on*  
397 *Health, Inference, and Learning*, pages 110–120, 2020.

## 398 A Proofs

### 399 A.1 Proof of Proposition 5

400 Define  $L^{(d)} := \ell(f(X), Y(d))$  for  $d \in \{0, 1\}$ . We begin by showing the first equality. By law of  
401 total expectation,

$$\psi = \mathbb{E}_T \left[ L^{(1)} \right] = \mathbb{E}_T \left[ \mathbb{E} \left[ L^{(1)} \mid R = 0, X \right] \right]. \quad (9)$$

402 By Assumption 2,

$$\mathbb{E}_T \left[ \mathbb{E} \left[ L^{(1)} | R = 0, X \right] \right] = \mathbb{E}_T \left[ \mathbb{E} \left[ L^{(1)} | R = 1, X \right] \right]. \quad (10)$$

403 By Assumption 1,

$$\mathbb{E}_T \left[ \mathbb{E} \left[ L^{(1)} | R = 1, X \right] \right] = \mathbb{E}_T \left[ \mathbb{E} \left[ L^{(1)} | R = 1, D = 1, X \right] \right] \quad (11)$$

404 By (2),

$$\mathbb{E}_T \left[ \mathbb{E} \left[ L^{(1)} | R = 1, D = 1, X \right] \right] = \mathbb{E}_T \left[ \mathbb{E} \left[ L | R = 1, D = 1, X \right] \right] \quad (12)$$

405 and the first equality follows by the definition of  $\mu$  and by combining (9)-(12).

406 To show the second equality, we start with  $\psi = \mathbb{E}_T [\mu(X)]$ . We begin by expressing this quantity as  
407 an integral over the covariate space and applying Assumption 4:

$$\psi = \int_{x \in \mathcal{X}} \mu(x) p_T(x) dx = \int_{x \in \mathcal{X}} \mu(x) \frac{p_T(x)}{p_S(x)} p_S(x) dx = \mathbb{E}_S \left[ \frac{p_T(X)}{p_S(X)} \mu(X) \right]. \quad (13)$$

408 By law of total expectation and by definition of  $R$ ,

$$\mathbb{E}_S \left[ \frac{p_T(X)}{p_S(X)} \mu(X) \right] = \mathbb{E}_S \left[ \frac{p_T(X)}{p_S(X)} \cdot \mathbb{E}[L | X, R = 1, D = 1] \right] = \mathbb{E}_S \left[ \frac{p_T(X)}{p_S(X)} \mathbb{E}_S[L | X, D = 1] \right]. \quad (14)$$

409 Observe that, by another application of law of total expectation,

$$\mathbb{E}_S [L | X, D = 1] = \frac{\mathbb{E}_S [DL | X]}{\mathbb{P}(D = 1 | X, R = 1)}. \quad (15)$$

410 Combining (13)-(15) yields

$$\psi = \mathbb{E}_S \left[ \frac{p_T(X)}{p_S(X)} \frac{\mathbb{E}_S [DL | X]}{\mathbb{P}(D = 1 | X, R = 1)} \right].$$

411 An application of the Tower Property and the definition of conditional probability yields the claim. ■

## 412 A.2 Candidate Influence Function Derivation

413 The following lemma recalls well-known results characterizing the influence functions of conditional  
414 expectation and density functions. See, e.g., [17].

415 **Lemma 7** (Auxiliary Influence Functions). *For the conditional loss function  $\mu(x)$ , its influence*  
416 *function  $\mathbb{IF} \{ \mu(X) \}$  is given by:*

$$\mathbb{IF} \{ \mu(x) \} = \frac{D \cdot R \cdot \mathbb{1}\{X = x\}}{\mathbb{P}(X = x, R = 1, D = 1)} (L - \mu(x)). \quad (16)$$

417 *Similarly, for the target covariate density  $p_T(x)$ , its influence function is given by:*

$$\mathbb{IF} \{ p_T(x) \} = \frac{1 - R}{\mathbb{P}(R = 0)} (\mathbb{1}\{X = x\} - p_T(x)). \quad (17)$$

418 **Lemma 8** (Target Risk Influence Function). *Define*

$$\varphi(Z; \mathbb{P}) = \frac{RD}{\pi(X)} \frac{g(X)}{\mathbb{P}(R = 0)} (L - \mu(X)) + \frac{1 - R}{\mathbb{P}(R = 0)} (\mu(X) - \psi(\mathbb{P})). \quad (18)$$

419 *Then  $\mathbb{E}_{\mathbb{P}} [\varphi(Z; \mathbb{P})] = 0$  and, for every one-dimensional parametric sub-model  $\mathbb{P}_\varepsilon = (1 - \varepsilon) \cdot \mathbb{P} + \varepsilon \bar{\mathbb{P}}$*   
420 *with score function  $s_\varepsilon$ ,*

$$\frac{\partial}{\partial \varepsilon} \psi(\mathbb{P}_\varepsilon) \Big|_{\varepsilon=0} = \mathbb{E}_{\mathbb{P}} [\varphi(Z; \mathbb{P}) s_\varepsilon(Z)].$$

421 *That is,  $\varphi(\cdot; \mathbb{P})$  is a influence function for  $\psi$ .*

422 **A.2.1 Proof of Proposition 6**

423 Following the semiparametric calculus of [17], we treat  $\mathcal{X}$  as a discrete set, apply Gateaux differenti-  
424 ation separately to each of  $\mu(\cdot)$  and  $p_T(\cdot)$ , and invoke the product rule for influence functions:

$$\mathbb{IF}\{\psi\} = \sum_{x \in \mathcal{X}} \mathbb{IF}\{\mu(x)\} p_T(x) + \sum_{x \in \mathcal{X}} \mu(x) \mathbb{IF}\{p_T(x)\}.$$

425 Applying the building block influence functions (16) and (17) given in Lemma 7 together with Bayes'  
426 Rule, we obtain:

$$\mathbb{IF}\{\psi\} = \frac{R \cdot D}{\pi(X)} \frac{g(x)}{\mathbb{P}(R=0)} (L - \mu(X)) + \frac{(1-R)}{\mathbb{P}(R=0)} (\mu(X) - \psi). \blacksquare$$

427 **A.3 von Mises Expansion**

428 **Lemma 9** (von Mises expansion). *For any two candidate laws  $\mathbb{P}$  and  $\bar{\mathbb{P}} \in \mathcal{P}$ , the mapping  $\psi : \mathcal{P} \rightarrow \mathbb{R}$   
429 admits the expansion*

$$\psi(\bar{\mathbb{P}}) - \psi(\mathbb{P}) = \int \varphi(z; \bar{\mathbb{P}}) d(\bar{\mathbb{P}} - \mathbb{P})(z) + R_2(\mathbb{P}, \bar{\mathbb{P}}) \quad (19)$$

430 where  $\varphi$  is as defined in (18) and the remainder term  $R_2(\mathbb{P}, \bar{\mathbb{P}})$  is given by

$$R_2(\mathbb{P}, \bar{\mathbb{P}}) = \int \frac{\bar{g}}{\bar{\rho}} \bar{\mu} \bar{\mathbb{P}} - \int \frac{g}{\rho} \mu \mathbb{P} + \int \frac{\bar{g}}{\bar{\rho}} \frac{\pi}{\bar{\pi}} (\mu - \bar{\mu}) \mathbb{P} + \frac{\rho}{\bar{\rho}} \int \frac{g}{\rho} \bar{\mu} \mathbb{P} - \int \frac{\rho}{\bar{\rho}} \frac{\bar{g}}{\bar{\rho}} \bar{\mu} \bar{\mathbb{P}}$$

431 where we have suppressed the arguments of functions in each term for brevity.

432 *Proof of Lemma 9.* For any two candidate laws  $\mathbb{P}$  and  $\bar{\mathbb{P}}$  on  $Z = (X, R, RD, RY)$ , the von Mises  
433 expansion of the estimand  $\psi$  around  $\mathbb{P}$  is given by:

$$\psi(\bar{\mathbb{P}}) - \psi(\mathbb{P}) = \int \varphi(z; \bar{\mathbb{P}}) d(\bar{\mathbb{P}} - \mathbb{P})(z) + R(\mathbb{P}, \bar{\mathbb{P}}) \quad (20)$$

434 where  $\varphi(z; \bar{\mathbb{P}})$  is a candidate influence function of  $\psi$  under  $\bar{\mathbb{P}}$  and  $R(\mathbb{P}, \bar{\mathbb{P}})$  is the remainder term  
435 which we will show is second-order. Since  $\varphi(z; \bar{\mathbb{P}})$  is centered under  $\bar{\mathbb{P}}$ , (20) can be rearranged to  
436 express the remainder term as:

$$R(\mathbb{P}, \bar{\mathbb{P}}) = \psi(\bar{\mathbb{P}}) - \psi(\mathbb{P}) + \int \varphi(z; \bar{\mathbb{P}}) d\mathbb{P}(z). \quad (21)$$

437 To evaluate the remainder, we express the influence function in terms of the nuisance terms  $\mu(X)$ ,  
438  $\pi(X)$ , and  $g(X)$  defined with respect to  $\mathbb{P}$  together with their counterparts  $\bar{\mu}(X)$ ,  $\bar{\pi}(X)$  and  $\bar{g}(X)$   
439 defined with respect to  $\bar{\mathbb{P}}$ .

440 We make use of the following two identities which hold for any measurable functions  $h(X, Y)$  and  
441  $h(X)$ , respectively:

$$\begin{aligned} \mathbb{E}_{\mathbb{P}}[RD \cdot h(X, Y)] &= \mathbb{E}_{\mathbb{P}}[\pi(X) \cdot h(X, Y)], \\ \mathbb{E}_{\mathbb{P}}[(1-R) \cdot h(X)] &= \mathbb{P}(R=0) \cdot \mathbb{E}_{\mathbb{P}}[h(X)|R=0]. \end{aligned}$$

442 Applying these identities to our remainder term allows us to express the integral term as follows:

$$\int \varphi(z; \bar{\mathbb{P}}) d\mathbb{P}(z) = \mathbb{E}_{\mathbb{P}} \left[ \frac{\bar{g}(X)}{\bar{\mathbb{P}}(R=0)} \frac{\pi(X)}{\bar{\pi}(X)} (\mu(X) - \bar{\mu}(X)) \right] + \frac{\mathbb{P}(R=0)}{\bar{\mathbb{P}}(R=0)} \left( \int \bar{\mu}(X) d\mathbb{P}(X|R=0) - \psi(\bar{\mathbb{P}}) \right). \quad (22)$$

443 By substituting the preceding integral term (22) into our expression for the remainder (21), we reach  
444 the expression:

$$R_2(\mathbb{P}, \bar{\mathbb{P}}) = \int \frac{\bar{g}}{\bar{\rho}} \bar{\mu} \bar{\mathbb{P}} - \int \frac{g}{\rho} \mu \mathbb{P} + \int \frac{\bar{g}}{\bar{\rho}} \frac{\pi}{\bar{\pi}} (\mu - \bar{\mu}) \mathbb{P} + \frac{\rho}{\bar{\rho}} \int \frac{g}{\rho} \bar{\mu} \mathbb{P} - \int \frac{\rho}{\bar{\rho}} \frac{\bar{g}}{\bar{\rho}} \bar{\mu} \bar{\mathbb{P}}$$

445 where we have suppressed the arguments from each nuisance function for compactness (i.e., we write  
446  $\mu$  for  $\mu(X)$ ). A series of algebraic manipulations yield the equivalent expression:

$$R_2(\mathbb{P}, \bar{\mathbb{P}}) = \int (\bar{\rho} - \rho) \frac{\bar{g}}{\bar{\rho}^2} \bar{\mu} \bar{\mathbb{P}} + \int (\rho - \bar{\rho}) \frac{g}{\rho \bar{\rho}} \mu \mathbb{P} + \int \frac{\bar{g}}{\bar{\rho}} \frac{(\pi - \bar{\pi})}{\bar{\pi}} (\mu - \bar{\mu}) \mathbb{P} + \int \frac{(\bar{g} - g)}{\bar{\rho}} (\mu - \bar{\mu}) \mathbb{P}.$$

447  $\square$

448 **B Estimation Details**

449 **B.1 Sample splitting nuisance function estimation**

450 Given  $n$  i.i.d. samples  $\mathcal{Z}_n := \{Z_i = (X_i, R_i, D_i, Y_i)\}_{i=1}^n$  where each  $Z_i$  is as in (1), we randomly  
 451 partition the index set  $\{1, \dots, n\}$  into  $K \geq 2$  disjoint folds  $\mathcal{I}_1, \dots, \mathcal{I}_K$  such that for each fold  $k$ ,  
 452  $|\mathcal{I}_k| \approx n/K$ . For each index  $i \in [n]$ , let  $k(i)$  denote the the fold containing the  $i$ -th observation. Then,  
 453 for each fold  $k$ , construct an empirical estimate of each nuisance function using only samples outside  
 454 of the  $k$ -th fold; Let  $\hat{\mu}^{(-k)}$ ,  $\hat{\pi}^{(-k)}$ , and  $\hat{g}^{(-k)}$  denote such held-out estimates of the functions  $\mu$ ,  $\pi$ ,  
 455 and  $g$ , respectively. Notice that, by construction, each of  $\hat{\mu}^{(-k)}$ ,  $\hat{\pi}^{(-k)}$ , and  $\hat{g}^{(-k)}$  are independent of  
 456 samples  $Z_i \in \mathcal{I}_k$ . Then, for each  $i \in [n]$ , set

$$\hat{\mu}_i = \hat{\mu}^{(-k(i))}(X_i), \quad \hat{\pi}_i = \hat{\pi}^{(-k(i))}(X_i), \quad \hat{g}_i = \hat{g}^{(-k(i))}(X_i),$$

457 that is, evaluate the plug-in estimate on the held-out sample. To estimate  $\rho$ , we simply take the full  
 458 sample mean:

$$\hat{\rho} = \frac{1}{n} \sum_{i=1}^n (1 - R_i).$$